PCCP

PAPER

View Article Online
View Journal | View Issue

Open Access Article. Published on 30 June 2025. Downloaded on 3/16/2026 4:00:36 PM.
This article is licensed under a Creative Commons Attribution 3.0 Unported Licence.

Check for updates

Cite this: *Phys. Chem. Chem. Phys.*, 2025, **27**, 16418

Unitary coupled-cluster theory for the electron propagator: electron attachment and physical properties *via* the intermediate state representation†

Manuel Hodecker, ‡[ab] Andreas Dreuw [a] and Adrian L. Dempwolff *[a]

A scheme for the calculation of electron-attachment (EA) processes within the framework of unitary coupled-cluster (UCC) theory is presented. Analogous to the description of electron-detachment, the intermediate state representation (ISR) approach is used for the formulation and its relation to the algebraic-diagrammatic construction scheme is pointed out. Due to the UCC ansatz, the resulting equations cannot be given by closed-form expressions, but need to be approximated. Explicit working equations for two computational schemes referred to as EA-UCC2 and EA-UCC3 are given, providing electron-attachment energies and spectroscopic amplitudes of electron-attached states dominated by one-particle excitations correct through second and third order in perturbation theory, respectively. In the derivation, an expansion of the UCC transformed Hamiltonian involving Bernoulli numbers as expansion coefficients is employed. In a benchmark against full configuration interaction (FCI) results including 50 states of 21 different species, both neutral and charged, closed- and open-shell, the novel methods are characterized by mean absolute errors of 0.15 eV (EA-UCC2) and 0.10 eV (EA-UCC3). Furthermore, an approach for the computation of physical properties of electron-attached as well as electron-detached states within the UCC framework is presented. It also builds upon the ISR approach, featuring an expectation value-like formulation similar to that of the equation-of-motion coupled-cluster (EOM-CC) method or the ISR approach of the algebraic-diagrammatic construction (ADC) method. Explicit expressions for the expectation value of a general one-particle operator correct through second order in perturbation theory are given and shown to be equivalent to those of the second-order ADC/ISR procedure.

Received 2nd April 2025,
Accepted 30th June 2025

DOI: 10.1039/d5cp01274k

rsc.li/pccp

1 Introduction

Molecular electron-attachment processes play a vital role in many fields of chemistry, biology, and materials science. Characterization of the resulting anions by means of the corresponding electron affinities (EAs), as well as properties of their electronic states,[1–3] is therefore of great interest and often indispensable in the development of, *e.g.*, organic photovoltaics or microelectronics.[4–6] In spite of their practical importance, many anions are very reactive and short-lived or metastable species,[7–9] making their experimental characterization cumbersome. The theoretical investigation of anionic species using high-level computational approaches is therefore inevitable, which due to effects such as orbital relaxation and electron correlation is not an easy task either.[10–12]

Computational schemes based on the electron propagator (or one-particle Green's function)[13] have been established in the study of ionization or electron-attachment spectra for many decades.[14–26] These approaches allow for direct computations of electron-attachment (or ionization) energies and spectral intensities, which is a clear advantage over the conceptually simpler "Δ-methods," where the N- and $(N+1)$-electron species are treated separately and the EA is successively computed by taking the difference between the two large total energies. The latter are generally feasible with all (open-shell) quantum-chemical methods, but apart from the aforementioned disadvantage of having to perform two

[a] *Interdisciplinary Center for Scientific Computing, Heidelberg University, Im Neuenheimer Feld 205, 69120 Heidelberg, Germany*
E-mail: dreuw@uni-heidelberg.de, adrian.dempwolff@iwr.uni-heidelberg.de
[b] *Division of Theoretical Chemistry and Biology, KTH Royal Institute of Technology, 100 44 Stockholm, Sweden*

† Electronic supplementary information (ESI) available: Computational details and a compiled listing of all individual EAs and corresponding pole strengths underlying the EA-UCC2 and EA-UCC3 statistical error evaluations. See DOI: https://doi.org/10.1039/d5cp01274k

‡ Present address: HQS Quantum Simulations GmbH, Rintheimer Str. 23, 76131 Karlsruhe, Germany.

 This journal is © the Owner Societies 2025

Open Access Article. Published on 30 June 2025. Downloaded on 3/16/2026 4:00:36 PM. This article is licensed under a Creative Commons Attribution 3.0 Unported Licence.

separate calculations, transition properties are not accessible, either.

In propagator methods, one can set out from the Dyson equation,[13,24] leading to schemes where the electron attachment ($\mathbf{G}^+$) and detachment ($\mathbf{G}^-$) parts of the electron propagator $\mathbf{G}(\omega)$ are coupled. Examples of Dyson approaches are the algebraic-diagrammatic construction (ADC) schemes,[19,24,27–29] the outer-valence Green's function (OVGF),[19,30,31] and the partial third-order approach (P3).[32,33] However, the coupling of the $\mathbf{G}^+$ and $\mathbf{G}^-$ parts is disadvantageous if one is interested in one of the parts only. Therefore, electron propagator methods have been developed, in which the Dyson equation is not employed and the $\mathbf{G}^+$ and $\mathbf{G}^-$ parts are treated separately. An example for such methods are the non-Dyson ADC schemes, which are also referred to as IP- and EA-ADC.[34,35] Explicit equations for the secular matrix and transition moments within the IP/EA-ADC schemes can be derived either *via* the original ADC procedure,[34] or purely algebraically, employing the intermediate state representation (ISR) concept[24,36–38] or an effective Liouvillian formalism.[39–41] The latter two approaches bear the additional advantage that they provide access to an explicitly constructable set of basis states, which allows for the calculation of final-state wave functions and from those one-electron density matrices and properties *via* a (generalized) expectation value.[35,42–46]

Another appealing feature of the ADC/ISR methods is that the resulting matrices are Hermitian and compact, the latter meaning that only a minimum number of explicit configuration classes are needed for a consistent n-th order treatment of transition and final-state properties.[34,38] Furthermore, ADC/ISR schemes are size consistent.[47]

Another family of methods is based on the equation-of-motion (EOM) coupled-cluster (CC) approach,[46,48–50] which can be seen as a non-Hermitian representation of the Hamiltonian within a basis of biorthogonal CC states.[51] The non-Hermitian eigenvalue problem of EOM-CC is prone to complex-valued solutions and the calculation of transition and state properties is complicated by the need to solve for two sets of left and right eigenvectors. However, they have the advantage of an iterative reference ground-state description *via* the corresponding CC scheme,[49,52] in contrast to the non-iterative Møller–Plesset (MP) ground state in ADC schemes.

The unitary coupled-cluster (UCC) approach[39,53–60] combines most of the advantages of the aforementioned ADC/ISR and EOM-CC methods. Moreover, UCC schemes bear the advantage over traditional (biorthogonal) CC approaches of possessing Hermitian symmetry, thus simplifying the calculation of transition and final-state properties. UCC approaches possess the same features of compactness and separability as the ADC schemes, the latter being a sufficient criterion to yield size-consistent results.[37,61] As a matter of fact, it was shown over a decade ago that a linear response UCC scheme correct through second order in MP perturbation theory is identical to ADC(2).[62] Recently, a UCC-based third-order formulation of the self-consistent polarization propagator was proposed[63] and shown to be closely related to the corresponding ADC scheme as well as to second-order CC-ADC schemes.[63–67] Successively, the UCC polarization propagator approach has been extended to the calculation of excited-state one-electron properties as well as core-excited states and X-ray absorption spectra.[68,69]

In a foregoing article,[61] the UCC approach has been applied to the $(N-1)$-electron part of the electron propagator, thus yielding ionization potentials (or, more generally, electron-detachment energies) and the corresponding transition amplitudes, and the approach has subsequently been benchmarked and compared to experimental and high-quality *ab initio* results.[70] The present article aims at extending this work and applying the same approach to the $(N+1)$-electron part of the electron propagator. For the formulation of the theory, we use again the ISR approach[36,37] and give explicit working equations for the secular matrix and effective transition moments of two schemes termed "EA-UCC2" and "EA-UCC3," which provide a description of electron-attached states of primary one-particle character correct through second and third order in MP perturbation theory (PT), respectively.

For a given system size N, the computational scaling associated with these schemes is N^6 for the iterative solution of the ground state amplitude equations for both UCC2 and UCC3, with a larger prefactor in the latter case. The self-consistent nature of the UCC ground state thus causes increased computational costs in comparison to the non-iterative MP ground state underlying the related EA-ADC methods, requiring one-step evaluations scaling as N^4 and N^6 in case of EA-ADC(2) and EA-ADC(3), respectively. It should be noted, though, that both the EA-UCC and EA-ADC schemes build upon electron repulsion integrals in molecular orbital representation, which have to be transformed from atomic orbitals in a single step scaling as N^5. That is, in case of EA-ADC(2), the computational scaling associated with the ground state calculation is, in fact, N^5. The ground state calculation is then followed by the iterative diagonalization of the respective EA-UCC matrix $\tilde{\tilde{\mathbf{M}}}$, which scales as N^4 and N^5 in case of EA-UCC2 and EA-UCC3, respectively, if a matrix-free diagonalization procedure is applied. For the diagonalization step, the computational scaling is thus identical to that of the EA-ADC(2) and EA-ADC(3) methods, respectively.

The performance of the novel EA-UCC schemes is assessed in a benchmark with respect to full configuration interaction (FCI) data. In addition, we present the working equations for the evaluation of one-particle properties of electron-attached as well as electron-detached states correct through second order in PT.

2 Theoretical methodology

For the development of unitary coupled-cluster (UCC) theory for electron attachment, we closely follow the methodology and notation used in ref. 61. In particular, the "Bernoulli expansion" for the similarity-transformed Hamiltonian is adopted.[63] The approach to electron-attachment energies is completely analogous to the one for ionization potentials or electron-

Open Access Article. Published on 30 June 2025. Downloaded on 3/16/2026 4:00:36 PM. This article is licensed under a Creative Commons Attribution 3.0 Unported Licence.

detachment energies.[61] However, it might be useful to go through the general theory in some detail before giving explicit working equations for a third-order scheme.

2.1 UCC approach to electron-attachment processes

An intermediate state representation (ISR) approach based on UCC has first been considered by Mukherjee and coworkers[39,56] and later reviewed by Mertins and Schirmer.[37] More recently, it has been employed for the calculation of neutrally excited and electron-detached species.[61,63–65,68–70] For the calculation of electron-attachment processes within this approach, $(N+1)$-electron EA-UCC states $\left|\tilde{\tilde{\Psi}}_J^{N+1}\right\rangle$ are defined according to

$$\left|\tilde{\tilde{\Psi}}_J^{N+1}\right\rangle = \mathrm{e}^{\hat{\sigma}}\hat{C}_J|\Phi_0\rangle, \tag{1}$$

where $|\Phi_0\rangle$ is the N-electron Hartree–Fock (HF) reference determinant, $\hat{\sigma} = \hat{S} - \hat{S}^\dagger$ is the cluster operator that parameterizes the UCC ground-state wave function $|\Psi_0^N\rangle = \mathrm{e}^{\hat{\sigma}}|\Phi_0\rangle$,[37,57,61] and $\hat{C}_J$ are electron-attachment operators that can be divided into one-particle (1p), two-particle-one-hole (2p1h), …, classes,

$$\hat{C}_J \in \{\hat{c}_a^\dagger; \hat{c}_b^\dagger\hat{c}_a^\dagger\hat{c}_i,\ a < b;\ \ldots\}. \tag{2}$$

Here and in the following we adopt the common convention of indices $i, j, \ldots$ denoting occupied orbitals in $|\Phi_0\rangle$, $a, b, \ldots$ denote unoccupied (virtual) ones, and $p, q, \ldots$ stand for the general case. The class of an arbitrary excitation J will be denoted by $[J]$. The EA-UCC intermediate states of eqn (1) thus correspond to a unitary transformation of the electron-attached HF determinants $|\Phi_J^{N+1}\rangle = \hat{C}_J|\Phi_0\rangle$, meaning they form a complete and orthonormal set.[37] The EA-UCC representation $\tilde{\tilde{\mathbf{H}}}$ of the Hamiltonian $\hat{H}$ is thus given by the matrix elements

$$\tilde{\tilde{H}}_{IJ} = \left\langle \tilde{\tilde{\Psi}}_I^{N+1}\middle|\hat{H}\middle|\tilde{\tilde{\Psi}}_J^{N+1}\right\rangle = \left\langle \Phi_I^{N+1}\middle|\bar{H}\middle|\Phi_J^{N+1}\right\rangle, \tag{3}$$

which can also be viewed as a representation of the UCC transformed Hamiltonian $\bar{H} = \mathrm{e}^{-\hat{\sigma}}\hat{H}\mathrm{e}^{\hat{\sigma}}$ within the basis of electron-attached CI configurations, $|\Phi_J^{N+1}\rangle \in \{|\Phi^a\rangle, |\Phi_i^{ab}\rangle, \ldots\}$, similar to EA-EOM-CC.[71] Correspondingly, the EA-UCC effective transition moments $\tilde{\tilde{\mathbf{f}}}$ are obtained from

$$\tilde{\tilde{f}}_{I,p} = \left\langle \tilde{\tilde{\Psi}}_I^{N+1}\middle|\hat{c}_p^\dagger\middle|\Psi_0\right\rangle = \left\langle \Phi_I^{N+1}\middle|\mathrm{e}^{-\hat{\sigma}}\hat{c}_p^\dagger\mathrm{e}^{\hat{\sigma}}\middle|\Phi_0\right\rangle. \tag{4}$$

The representation of the Hamiltonian within the set of EA-UCC states in eqn (3), or rather its shifted version $\tilde{\tilde{\mathbf{M}}}$ defined as

$$\tilde{\tilde{M}}_{IJ} = \tilde{\tilde{H}}_{IJ} - E_0^N\delta_{IJ}, \tag{5}$$

gives rise to a Hermitian eigenvalue equation

$$\tilde{\tilde{\mathbf{M}}}\,\mathbf{Y} = \mathbf{Y}\boldsymbol{\Omega}, \quad \mathbf{Y}^\dagger\mathbf{Y} = \mathbf{1}, \tag{6}$$

which yields negative vertical electron-attachment energies as eigenvalues $\omega_n = E_n^{N+1} - E_0^N$ collected in the diagonal matrix $\boldsymbol{\Omega}$ and the corresponding eigenvectors collected in the columns of $\mathbf{Y}$. Transition probabilities can be deduced from the spectroscopic amplitudes $\mathbf{x}$, whose elements are given by

$$x_{n,q} = \langle\Psi_n^{N+1}|\hat{c}_q^\dagger|\Psi_0^N\rangle, \tag{7}$$

where $|\Psi_n^{N+1}\rangle$ are the exact electron-attached states. They can be obtained from the effective transition moments $\tilde{\tilde{\mathbf{f}}}$ *via* $\mathbf{x} = \mathbf{Y}^\dagger\tilde{\tilde{\mathbf{f}}}$.[34,37]

The exact electron-attached states $|\Psi_n^{N+1}\rangle$ can then be written in terms of the intermediate states as

$$\left|\Psi_n^{N+1}\right\rangle = \sum_J Y_{Jn}\left|\tilde{\tilde{\Psi}}_J^{N+1}\right\rangle, \tag{8}$$

which means that the elements of the eigenvectors $Y_{In} = \left\langle\tilde{\tilde{\Psi}}_I^{N+1}\middle|\Psi_n^{N+1}\right\rangle$ are the expansion coefficients of the exact electron-attached states in the intermediate state basis.

A different approach to the calculation of electron-attachment energies and relative spectral intensities is based on the one particle Green's function or electron propagator $\mathbf{G}(\omega) = \mathbf{G}^-(\omega) + \mathbf{G}^+(\omega)$. Considering only the $(N+1)$-electron part $\mathbf{G}^+(\omega)$, corresponding to the non-Dyson approach to the electron propagator,[34] its spectral representation is given as[24]

$$G_{pq}{}^+(\omega) = \sum_n \frac{\left\langle\Psi_0^N\middle|\hat{c}_p\middle|\Psi_n^{N+1}\right\rangle\left\langle\Psi_n^{N+1}\middle|\hat{c}_q^\dagger\middle|\Psi_0^N\right\rangle}{\omega + E_0^N - E_n^{N+1}}, \tag{9}$$

where the elements of the spectroscopic amplitudes $\mathbf{x}$ from eqn (7) appear as factors in the residues. By employing the definition of the UCC ground state, and a resolution of the identity in terms of EA-UCC states from eqn (1), the same secular equation as with the ISR approach is obtained, analogous to the polarization propagator case.[37,63]

Furthermore, it should be mentioned that that same properties such as compactness and separability apply to the EA-UCC as for the IP-UCC scheme.[61]

2.2 The EA-UCC3 scheme

In analogy to the treatment of the $(N-1)$-electron part of the electron propagator within the UCCSD truncation scheme ($\hat{\sigma} = \hat{\sigma}_1 + \hat{\sigma}_2$),[61] electron-attachment energies are obtained by diagonalizing the $\bar{H}$ matrix shifted by the ground-state energy E_0^N within the space comprising 1p and 2p1h configurations. For electron-attachment energies of states with predominantly 1p character to be correct through third order in terms of MP perturbation theory, the 1p/1p block needs to be correct through third order, the 1p/2p1h and 2p1h/1p coupling blocks through second order and the 2p1h/2p1h block through first order. This scheme is then termed EA-UCC3. The somewhat simpler second-order EA-UCC2 scheme is obtained by dropping the respective highest-order terms in each block. Using the definition of the second- and third-order Hamiltonians $\bar{H}^{\mathrm{UCC2}}$ and $\bar{H}^{\mathrm{UCC3}}$ in eqn (8) and (9) of ref. 61, respectively, yields the following terms with leading contributions up to third order in

Open Access Article. Published on 30 June 2025. Downloaded on 3/16/2026 4:00:36 PM.
This article is licensed under a Creative Commons Attribution 3.0 Unported Licence.

the 1p/1p block $\tilde{\tilde{M}}_{a,b}$,

$$\tilde{\tilde{M}}_{a,b} = \langle \Phi^a | \bar{H}^{\mathrm{UCC3}} - E_0^N | \Phi^b \rangle \tag{10a}$$

$$\begin{aligned} &= F_{ab} - \frac{1}{4}\left(\sum_{ijc} \langle ij\|ca\rangle s_{ijcb} + \text{h.c.}\right) \\ &\quad + \left(\sum_{ic} \langle ai\|bc\rangle s_{ic} + \text{h.c.}\right) \\ &\quad + \left(\left(-\frac{1}{2}\sum_{ijkcd} \langle id\|bk\rangle s_{ijac} s^*_{jkcd} \right.\right. \\ &\quad \left.\left. - \frac{1}{8}\sum_{ijcde} \langle cd\|be\rangle s_{ijae} s^*_{ijcd}\right) + \text{h.c.}\right) \\ &\quad + \frac{1}{2}\sum_{ijcde} \langle ad\|be\rangle s^*_{ijcd} s_{ijce} \\ &\quad - \frac{1}{2}\sum_{ijkcd} \langle aj\|bk\rangle s_{ijcd} s^*_{ikcd}, \end{aligned} \tag{10b}$$

where the F_{pq} denote Fock matrix elements, $\langle pq\|rs\rangle$ anti-symmetrized two-electron integrals in physicists' ("1212") notation,[72] and "h.c." stands for the Hermitian conjugate. The 1p/2p1h coupling block $\tilde{\tilde{M}}_{a,ibc}$ with leading terms up to second order is given as

$$\tilde{\tilde{M}}_{a,ibc} = \langle \Phi^a | \bar{H}^{\mathrm{UCC2}} | \Phi_i^{bc} \rangle \tag{11a}$$

$$\begin{aligned} &= -\langle cb\|ai\rangle + \frac{1}{2}\sum_{jk} \langle ai\|jk\rangle s^*_{jkbc} \\ &\quad + \hat{\mathscr{P}}(bc)\sum_{jd} \langle ad\|bj\rangle s^*_{ijcd}, \end{aligned} \tag{11b}$$

where $\hat{\mathscr{P}}(pq) = 1 - \hat{P}_{pq}$ anti-symmetrizes the following expression with respect to indices p and q, and the 2p1h/1p coupling block is the Hermitian conjugate of this one. Finally, the 2p1h/2p1h block with leading terms through first order is given as

$$\tilde{\tilde{M}}_{iab,jcd} = \left\langle \Phi_i^{ab} \middle| \hat{H} - E_0^N \middle| \Phi_j^{cd} \right\rangle \tag{12a}$$

$$\begin{aligned} &= F_{ac}\delta_{bd}\delta_{ij} + F_{bd}\delta_{ac}\delta_{ij} - F_{ji}\delta_{ac}\delta_{bd} \\ &\quad + \delta_{ij}\langle ab\|cd\rangle \\ &\quad - \hat{\mathscr{P}}(cd)(\delta_{bd}\langle ic\|ja\rangle + \delta_{ac}\langle jb\|id\rangle). \end{aligned} \tag{12b}$$

In the second-order EA-UCC2 scheme, only the first two terms of eqn (10b), the bare two-electron integral of eqn (11b), and only the Fock matrix elements of eqn (12b) are the constituting ingredients.

2.3 EA-UCC effective transition moments

The EA-UCC effective transition moments $\tilde{\tilde{\mathbf{f}}}$ are obtained according to eqn (4) and can be divided according to the excitation class $[I]$ of the intermediate state and then further into a particle and a hole part depending on the orbital index p.

Starting with $[I]$ being a 1h excitation, the 1p/h part $\tilde{\tilde{f}}_{a,i}$ can be shown to be identical, apart from a sign change due to the different order of the second-quantized operators, to the corresponding 1h/p part of the IP-UCC scheme through third order.[61] This means that it can be written through double commutators or third order as a projection onto singly exicted determinants,

$$\begin{aligned} \tilde{\tilde{f}}_{a,i} &= \left\langle \tilde{\tilde{\Psi}}_a^{N+1} \middle| \hat{c}_i^\dagger \middle| \Psi_0 \right\rangle = \left\langle \Phi^a \middle| e^{-\hat{\sigma}} \hat{c}_i^\dagger e^{\hat{\sigma}} \middle| \Phi_0 \right\rangle \\ &= \left\langle \Phi^a \middle| \hat{c}_i^\dagger + \left[\hat{c}_i^\dagger, \hat{\sigma}\right] + \frac{1}{2}\left[\left[\hat{c}_i^\dagger, \hat{\sigma}\right], \hat{\sigma}\right] + \cdots \middle| \Phi_0 \right\rangle \\ &= -\left\langle \Phi_i^a \middle| \hat{S} + \frac{1}{2}\hat{S}^\dagger \hat{S} \middle| \Phi_0 \right\rangle + \mathscr{O}(4), \end{aligned} \tag{13}$$

where $\mathscr{O}(n)$ stands for all terms of n-th and higher order. Accordingly, in a consistent third-order scheme it would be given by

$$\begin{aligned} \tilde{\tilde{f}}_{a,i} &= -\left\langle \Phi_i^a \middle| \hat{S}_1 + \frac{1}{2}\hat{S}_1^\dagger \hat{S}_2 + \frac{1}{2}\hat{S}_2^\dagger \hat{S}_3 \middle| \Phi_0 \right\rangle + \mathscr{O}(4) \\ &= -s_{ia} - \frac{1}{2}\sum_{jb} s^*_{jb} s_{ijab} - \frac{1}{8}\sum_{jkbc} s^*_{jkbc} s_{ijkabc} + \mathscr{O}(4). \end{aligned} \tag{14}$$

It should be noted that in the present approximate UCCSD scheme, the last term including the $\hat{S}_3$ operator does not occur. However, neglecting this term does not affect the third-order consistency, as was shown for the analogous case of IP-UCC in ref. 61.

Correspondingly, the 1p/p block $\tilde{\tilde{f}}_{a,b}$ is given by

$$\begin{aligned} \tilde{\tilde{f}}_{a,b} &= \left\langle \tilde{\tilde{\Psi}}_a^{N+1} \middle| \hat{c}_b^\dagger \middle| \Psi_0 \right\rangle = \left\langle \Phi^a \middle| e^{-\hat{\sigma}} \hat{c}_b^\dagger e^{\hat{\sigma}} \middle| \Phi_0 \right\rangle \\ &= \delta_{ab} - \frac{1}{4}\sum_{ijc} s^*_{ijac} s_{ijbc} + \mathscr{O}(4). \end{aligned} \tag{15}$$

Let us proceed to the case where $[I]$ corresponds to a 2h1p excitation. Analogous to the 1p/h block, the 2p1h/h block can be written as a projection onto doubly excited determinants, which in this case is sufficient through fourth order in

Open Access Article. Published on 30 June 2025. Downloaded on 3/16/2026 4:00:36 PM.
This article is licensed under a Creative Commons Attribution 3.0 Unported Licence.

perturbation theory,

$$\begin{aligned}\tilde{\tilde{f}}_{iab,j} &= \left\langle \tilde{\tilde{\Psi}}^{N+1}_{iab} \middle| \hat{c}_j^\dagger \middle| \Psi_0 \right\rangle = \left\langle \Phi_i^{ab} \middle| e^{-\hat{\sigma}} \hat{c}_j^\dagger e^{\hat{\sigma}} \middle| \Phi_0 \right\rangle \\ &= -\left\langle \Phi_{ij}^{ab} \middle| \hat{S} + \frac{1}{2}\hat{S}^\dagger \hat{S} \middle| \Phi_0 \right\rangle + \mathcal{O}(5) \\ &= -\left\langle \Phi_{ij}^{ab} \middle| \hat{S}_2 + \frac{1}{2}\hat{S}_1^\dagger \hat{S}_3 \middle| \Phi_0 \right\rangle + \mathcal{O}(5) \\ &= -s_{ijab} - \frac{1}{2}\sum_{kc} s_{kc}^* s_{ijkabc} + \mathcal{O}(5) \\ &= -s_{ijab} + \mathcal{O}(4).\end{aligned} \tag{16}$$

Let us note that this finding makes eqn (E4b) of ref. 61 somewhat more stringent. Finally, the 2p1h/p block vanishes through second order,

$$\begin{aligned}\tilde{\tilde{f}}_{iab,c} &= \left\langle \tilde{\tilde{\Psi}}^{N+1}_{iab} \middle| \hat{c}_c^\dagger \middle| \Psi_0 \right\rangle = \left\langle \Phi_i^{ab} \middle| e^{-\hat{\sigma}} \hat{c}_c^\dagger e^{\hat{\sigma}} \middle| \Phi_0 \right\rangle \\ &= \frac{1}{2}\left\langle \Phi_i^{ab} \middle| \hat{S}_1^\dagger \hat{S}_2 \hat{c}_c^\dagger - \hat{c}_c^\dagger \hat{S}_1^\dagger \hat{S}_2 \middle| \Phi_0 \right\rangle + \mathcal{O}(4) \\ &= \frac{1}{2}\sum_j s_{jc}^* s_{ijab} \\ &\quad + \frac{1}{2}\hat{\mathscr{P}}(ab)\delta_{bc}\sum_{jd} s_{jd}^* s_{ijad} + \mathcal{O}(4) \\ &= 0 + \mathcal{O}(3),\end{aligned} \tag{17}$$

as needed for the EA-UCC3 scheme, but has non-vanishing contributions starting in third order, unlike the corresponding block of the EA-ADC scheme, which vanishes in all orders of perturbation theory.[34,45,61]

2.4 One-electron properties of molecular electron-detached and -attached states

Physical properties of electron-detached or electron-attached states other than the energy can be calculated as the expectation value of the operator $\hat{D}$ corresponding to the observable with the wave function,

$$D_n = \langle \Psi_n^{N\pm1} | \hat{D} | \Psi_n^{N\pm1} \rangle. \tag{18}$$

In the following, $\hat{D}$ is a general one-electron operator given in second quantization as

$$\hat{D} = \sum_{pq} d_{pq} \hat{c}_p^\dagger \hat{c}_q, \tag{19}$$

where $d_{pq} = \langle \phi_p | \hat{d} | \phi_q \rangle$ are the one-electron matrix elements associated with $\hat{D}$ in the MO basis.

Within the UCC/ISR approach, this expectation value can be calculated by plugging the respective wave-function expansion according to that of eqn (8) twice into the general expectation value (18), D_n (for $n > 0$) is obtained from

$$D_n = \sum_{IJ} Y_{n,I}^* \tilde{\tilde{D}}_{IJ} Y_{n,J} = \mathbf{Y}_n^\dagger \tilde{\tilde{\mathbf{D}}} \mathbf{Y}_n, \tag{20}$$

from the n-th eigenvector $\mathbf{Y}_n$ of the UCC secular problem and the matrix $\tilde{\tilde{\mathbf{D}}}$, which is the representation of $\hat{D}$ within the basis of UCC intermediate states,

$$\tilde{\tilde{D}}_{IJ} = \left\langle \tilde{\tilde{\Psi}}_I^{N\pm1} \middle| \hat{D} \middle| \tilde{\tilde{\Psi}}_J^{N\pm1} \right\rangle. \tag{21}$$

Analogously, one may compute transition moments between two different states ($n \neq m$) according to

$$T_{nm} = \langle \Psi_n^{N\pm1} | \hat{D} | \Psi_n^{N\pm1} \rangle = \mathbf{Y}_n^\dagger \tilde{\tilde{\mathbf{D}}} \mathbf{Y}_m. \tag{22}$$

One may now rewrite the elements of $\tilde{\tilde{\mathbf{D}}}$ by inserting the definition of the $N \pm 1$ UCC states analoguous to eqn (1) to obtain

$$\tilde{\tilde{D}}_{IJ} = \left\langle \Phi_0 \middle| \hat{C}_I^\dagger e^{-\hat{\sigma}} \hat{D} e^{\hat{\sigma}} \hat{C}_J \middle| \Phi_0 \right\rangle = \langle \Phi_I^{N\pm1} | \bar{D} | \Phi_J^{N\pm1} \rangle, \tag{23}$$

which can be seen as matrix elements of the transformed operator $\bar{D}$,[68]

$$\bar{D} = e^{-\hat{\sigma}} \hat{D} e^{\hat{\sigma}} = \hat{D} + [\hat{D}, \hat{\sigma}] + \frac{1}{2!}\left[[\hat{D}, \hat{\sigma}], \hat{\sigma}\right] + \cdots, \tag{24}$$

within the basis of ($N \pm 1$)-electron determinants, $|\Phi_J^{N\pm1}\rangle = \hat{C}_J|\Phi_0\rangle$. Explicit matrix elements for a consistent second-order description of $\tilde{\tilde{\mathbf{D}}}$ are given in Appendix A. It should be mentioned that this formulation of excitation energies, transition moments and excited-state properties is separable for a system consisting of two noninteracting fragments and thus yields size-intensive results.[37,42,47]

3 Computational details

The EA-UCC calculations presented in this work were performed using development versions of the Q-Chem 5 software.[73] Therein, EA-UCC methods were implemented in the adcman module,[74] exploiting the libtensor library[75] and the existing infrastructure to perform ground-state UCC3[65] calculations.

For the benchmark study of the EA-UCC2 and EA-UCC3 methods presented in Section 4, the benchmark data set introduced in ref. 45 was employed. A detailed listing of the molecular geometries and basis sets used is given in Section S1 of the ESI.† Statistical error estimates were computed with respect to FCI data available in ref. 45. The benchmark data set consists of 50 electron-attached states in 21 different electronic systems, comprising both neutral and charged, as well as closed- and open-shell molecular species.

It shall be noted that, especially in the case of neutral species, the benchmark data set also includes states which are electronically unbound. The corresponding computed EAs are thus highly basis set dependent, as they belong to either electronic resonances or even wrongly discretized continuum states. The objective of the present study is, however, an assessment how well the presented EA-UCC schemes are converged with respect to FCI results for a given basis set. The computed error characteristics can therefore be expected to

Open Access Article. Published on 30 June 2025. Downloaded on 3/16/2026 4:00:36 PM.
This article is licensed under a Creative Commons Attribution 3.0 Unported Licence.

provide a comprehensive picture of the EA-UCC method performance.

4 Results and discussion

Here, we present an assessment of the accuracy and precision of the novel EA-UCC2 and EA-UCC3 methods. For this purpose, we employ the FCI benchmark data set for electron-attached states first introduced in ref. 45 in the context of EA-ADC, covering closed- and open-shell species of different categories. Among the molecules with closed-shell initial states are neutral molecules (N) and cations (C). The open-shell species comprise neutral radicals with doublet ground states (NR), neutral molecules in their lowest triplet-excited states (T_1) and radical cations with doublet ground states (RC).

Among all states available in the FCI benchmark data set, only those exposing pole strengths $P > 0.6$ were considered for the statistical error evaluation. That is, electron-attached states mainly described by two-particle-one-hole (2p1h) transitions were exempted. Such states appear for different reasons. Apart from actual 2p1h transitions leading to "satellite states", a one-particle (1p) state may, on a specific level of theory, "accidentally" mix with close-lying 2p1h states, in which case an unambiguous assignment to FCI states is not possible. Such states can be found for electron attachment to closed- and open-shell initial states and are characterized by considerably decreased pole strengths.

For electron attachment to open-shell systems, another source of increased 2p1h character has to be considered as well. The issue may be demonstrated at the example of electron attachment to doublet reference states characterized by $M_S = \frac{1}{2}$. This is done in Fig. 1, which provides a schematical overview of all three possible 1p processes (denoted A, B and C). In contrast to processes A and B, which generate well-defined $\hat{S}^2$-adapted final states, transition C leads to an open-shell species which needs to be linearly combined with a second configuration in order to form an $\hat{S}^2$-adapted electron-attached state. The missing configuration is indeed accessible by means of a 2p1h transition (denoted D in Fig. 1). However, this implies a mixing of different types of configurations which, in EA-UCC methods, are not described on equal theoretical footing. More generally, the excitation manifold used for the EA-UCC matrix representation may even be incomplete for a full recovery of spin symmetry in electron-attached states, as has been discussed in ref. 76 in the context of electron number-conserving excitations. Results computed for this kind of states should thus be interpreted carefully and will, in the present context, not be considered further. As in the case of "accidental" mixing of 1p and 2p1h states, the respective states are easily identified as states in which strong mixing of 1p and 2p1h configurations occurs, which, in turn, is reflected in considerably decreased pole strengths.

The results of our benchmark calculations are presented in Table 1. Starting with the closed-shell systems, the overall accuracy computed for 35 EA-UCC2 states is characterized by

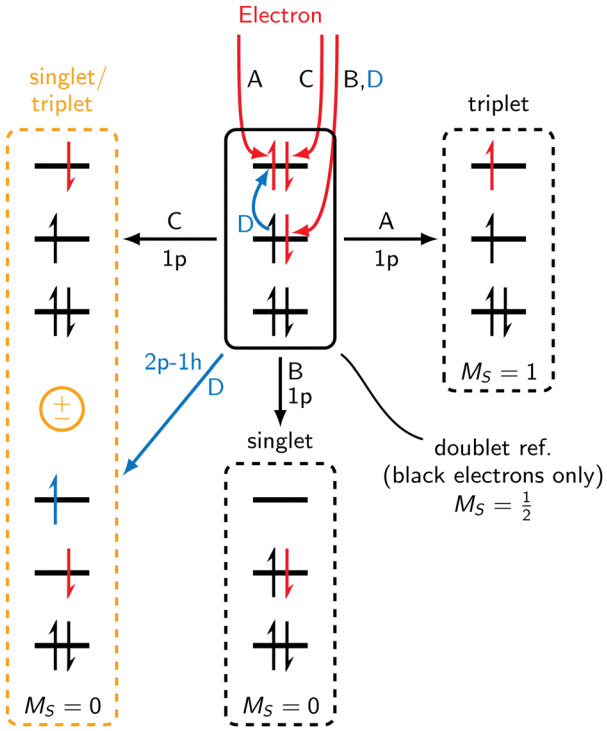

Fig. 1 Schematic representation of possible final electronic configurations accessible through 1p-type electron attachment transitions from an open-shell doublet reference. The open-shell singlet and triplet states characterized by $M_S = 0$ (orange box) require a combination of 1p and 2p1h configurations in order to be $\hat{S}^2$ eigenfunctions. Electrons of the reference determinant are shown in black, those added during the attachment process in red, and electrons excited from the reference determinant during the attachment process in blue.

a mean absolute error (MAE) of 0.12 eV, while the mean signed error (MSE) and its standard deviation (SDE) are MSE ± SDE = −0.02 ± 0.18 eV. Here, the maximum absolute deviation is found for the $2^2\Sigma^+$ state of the HCN anion, Δ_{max} = 0.60 eV (see ESI† for a detailed listing of the individual states underlying the statistical evaluation). For EA-UCC3 (34 states), the respective error characteristics are MAE = 0.05 eV and MSE ± SDE = 0.00 ± 0.10 eV. The maximum absolute deviation from FCI reference data is again found for the $2^2\Sigma^+$ state of the HCN anion, however, compared to EA-UCC2 this value is reduced to now only Δ_{max} = 0.41 eV. The individual error estimates, in particular the MAE and SDE, computed for neutral (25/24 EA-UCC2/EA-UCC3 states) and cationic (10/10 states) initial systems are in line with the respective values computed for the complete closed-shell set. However, the EA-UCC2 and EA-UCC3 mean signed errors of −0.11 and −0.04 eV found for cationic initial states indicate that for this kind of systems EAs are consistently underestimated by EA-UCC methods. In contrast, such a behavior is not observed for neutral initial states, where an MSE of 0.02 eV is found for both EA-UCC2 and EA-UCC3.

Turning now to open-shell systems, the accuracy and precision is generally reduced compared to closed-shell initial states. For EA-UCC2, the mean absolute error computed for 16 electron-attached states is MAE = 0.22 eV, and thus close to

Open Access Article. Published on 30 June 2025. Downloaded on 3/16/2026 4:00:36 PM.
This article is licensed under a Creative Commons Attribution 3.0 Unported Licence.

Table 1 Mean absolute error (MAE), mean signed error (MSE) and its standard deviation (SDE), as well as the maximum absolute error (Δ_{max}) of vertical EAs of closed- and open-shell systems computed for EA-UCC2 and EA-UCC3 with respect to FCI reference data from ref. 45. The closed-shell systems comprise neutral molecules (N) and cations (C), and the open-shell systems comprise neutral radicals (NR), molecules in the lowest-triplet excited state (T_1), and radical cations (RC). Only 1p-type electron attachment transitions with pole strengths $P > 0.6$ have been taken into account. The number k of states considered for each set of states is given in parantheses in the first column as (k_{UCC2}/k_{UCC3}). A compiled listing of all individual EAs is available in the ESI

Initial system	Error	EA-UCC2	EA-UCC3
Closed-shell			
N (25/24)	MAE	0.12	0.06
	MSE	0.02	0.02
	SDE	0.19	0.12
	Δ_{max}	0.60	0.41
C (10/10)	MAE	0.11	0.04
	MSE	−0.11	−0.04
	SDE	0.16	0.05
	Δ_{max}	0.39	0.13
Overall closed-shell (35/34)	MAE	0.12	0.05
	MSE	−0.02	0.00
	SDE	0.18	0.10
	Δ_{max}	0.60	0.41
Open-shell			
NR (4/4)	MAE	0.25	0.20
	MSE	0.09	−0.02
	SDE	0.36	0.27
	Δ_{max}	0.68	0.40
T_1 (6/6)	MAE	0.28	0.29
	MSE	−0.27	−0.28
	SDE	0.43	0.43
	Δ_{max}	0.99	0.79
RC (6/6)	MAE	0.16	0.12
	MSE	−0.09	−0.12
	SDE	0.26	0.19
	Δ_{max}	0.60	0.35
Overall open-shell (16/16)	MAE	0.22	0.20
	MSE	−0.11	−0.16
	SDE	0.36	0.32
	Δ_{max}	0.99	0.79
Overall (51/50)	MAE	0.15	0.10
	MSE	−0.05	−0.05
	SDE	0.25	0.20
	Δ_{max}	0.99	0.79

the MAE of 0.20 eV found for EA-UCC3 (16 states). EA-UCC2 shows an underestimation of EAs characterized by an MSE of −0.11 eV. This trend is even more pronounced for EA-UCC3 (MSE = −0.16 eV). However, the error spread slightly reduces from EA-UCC2 (SDE = 0.36 eV) to EA-UCC3 (SDE = 0.32 eV). The reduced precision of EAs computed with open-shell references is also reflected in the maximum absolute deviations from FCI results. For EA-UCC2, the respective value of Δ_{max} = 0.99 eV is observed for the $1^2\Sigma^+$ state of the LiH anion when a triplet-excited (T_1) LiH* reference state is employed. For EA-UCC3, it is Δ_{max} = 0.79 eV in case of the 1^2A state of the NH_3 anion when, again, a triplet-excited NH_3* reference state is employed. However, it should be noted that the error characteristics computed for the different categories of open-shell initial states are less meaningful than those computed for their closed-shell counterparts due to the relatively small number of states considered in our benchmark set (NR: 4 states, T_1: 6 states, and RC: 6 states for both EA-UCC2 and EA-UCC3).

Taking together the closed- and open-shell systems, EA-UCC3 slightly outperforms EA-UCC2 in terms of accuracy as well as precision: for 50 EA-UCC3 states, the error characteristics are given by MAE = 0.10 eV and MSE ± SDE = −0.05 ± 0.20 eV; for EA-UCC2, they are MAE = 0.15 eV and MSE ± SDE = −0.05 ± 0.25 eV. Also, the maximum absolute deviation is smaller in case of EA-UCC3 (Δ_{max} = 0.79 eV) than in case of EA-UCC2 (Δ_{max} = 0.99 eV).

5 Summary and conclusions

Two computational schemes for the calculation of molecular electron attachment energies based on a unitary coupled cluster approach have been derived and implemented in the Q-Chem quantum-chemical software package.[73] These EA-UCC2 and EA-UCC3 methods yield results which are consistent through second and third order of Møller–Plesset perturbation theory, respectively, for electronic states accessible in one-particle processes. In addition, second-order schemes for the calculation of molecular one-electron properties of electron-attached and electron-detached states have been derived and are presented in Appendix A.

The accurracy and precision of the EA-UCC2 and EA-UCC3 schemes for the calculation of electron attachment energies was assessed in a benchmark study with respect to FCI results for 50 electron-attached states in 21 different molecular open- and closed-shell species. As already observed for the EA-ADC methods,[45] the improvement of the third-order scheme over the second-order scheme is not as pronounced as in the case of IP-UCC.[70] For closed-shell systems, the EA-UCC2 and EA-UCC3 schemes are characterized by mean absolute errors of 0.12 and 0.05 eV, respectively. For open-shell systems, generally larger errors are observed, being 0.22 and 0.20 eV for EA-UCC2 and EA-UCC3, respectively. One possible reason for the lower accurracy observed for open-shell systems is spin contamination, as has been pointed out recently in the context of IP- and EA-ADC[77] as well as ADC for electron number-conserving excitations.[76]

Author contributions

Manuel Hodecker: conceptualization, investigation, methodology, software, validation, writing – original draft; Andreas Dreuw: conceptualization, funding acquisition, project administration, resources, supervision, writing – review and editing; Adrian L. Dempwolff: conceptualization, data curation, formal analysis, investigation, software, validation, visualization, writing – original draft, writing – review and editing.

Conflicts of interest

There are no conflicts of interest to declare.

Data availability

The data that supports the findings of this study are available within the article and its ESI.†

 This journal is © the Owner Societies 2025

Open Access Article. Published on 30 June 2025. Downloaded on 3/16/2026 4:00:36 PM.
This article is licensed under a Creative Commons Attribution 3.0 Unported Licence.

Appendix

A Second-order ($N \pm 1$)-electron UCC expressions of one-particle operators

In the following, explicit expressions for the matrix elements of a general one-particle operator

$$\hat{D} = \sum_{pq} d_{pq} \hat{c}_p^\dagger \hat{c}_q \tag{25}$$

for a consistent second-order description are presented. The general form of the matrix elements is given by

$$\tilde{\tilde{D}}_{IJ} = \left\langle \tilde{\tilde{\Psi}}_I^{N\pm1} \middle| \hat{D} \middle| \tilde{\tilde{\Psi}}_J^{N\pm1} \right\rangle = \langle \Phi_I^{N\pm1} | \bar{D} | \Phi_J^{N\pm1} \rangle, \tag{26}$$

where the similarity-transformed operator $\bar{D}$ is defined in eqn (24). As before, the indices $i, j, k, \ldots$ and $a, b, c, \ldots$ refer to unoccupied (virtual) and occupied orbitals, respectively, while $p, q, r, \ldots$ are used for the general case. The ground-state contribution D_0 is implicitly subtracted in the following.

A.1 ($N - 1$)-electron case

A.1.1 h/h block. The zeroth-order part is given by

$$\langle \Phi_i | \hat{D} | \Phi_j \rangle = -d_{ij}, \tag{27}$$

while for a valid HF reference there is no first-order contribution. The second-order contribution from the single commutator involving $\hat{\sigma}_1$ is given by

$$\langle \Phi_i | [\hat{D}, \hat{\sigma}_1] | \Phi_j \rangle = -\sum_c \left(d_{ic} s_{jc} + d_{cj} s_{ic}^* \right). \tag{28}$$

The different contributions stemming from the double commutator involving $\hat{\sigma}_2$ are given by

$$\begin{aligned} \langle \Phi_i | [[\hat{D}, \hat{\sigma}_2], \hat{\sigma}_2] | \Phi_j \rangle = & -\frac{1}{4} \sum_{klcd} d_{jk} s_{klcd}^* s_{ilcd} \\ & -\frac{1}{4} \sum_{klcd} d_{ki} s_{jlcd}^* s_{klcd} \\ & -\sum_{kcde} d_{cd} s_{kjce}^* s_{kide} \\ & +\frac{1}{2} \sum_{klcd} d_{lk} s_{kjcd}^* s_{licd}. \end{aligned} \tag{29}$$

A.1.2 h/2h1p block. For the coupling block, the zeroth-order contribution is given by

$$\langle \Phi_i | \hat{D} | \Phi_{jk}^b \rangle = \delta_{ik} d_{jc} - \delta_{ij} d_{kc}, \tag{30}$$

while the first-order contributions are given by

$$\begin{aligned} \left\langle \Phi_i^a \middle| [\hat{D}, \hat{\sigma}_2] \middle| \Phi_{jk}^{bc} \right\rangle = & \delta_{ij} \sum_{ld} d_{dl} s_{lkdb}^* - \delta_{ik} \sum_{ld} d_{jb} s_{ljdb}^* \\ & + \sum_d d_{di} s_{jkdb}^*. \end{aligned} \tag{31}$$

The other coupling block is the Hermitian conjugate of this one.

A.1.3 2h1p/2h1p block. This block is only needed in zeroth order, where the corresponding terms are given by

$$\begin{aligned} \left\langle \Phi_{ij}^a \middle| \hat{D} \middle| \Phi_{kl}^c \right\rangle = & \delta_{ik} \delta_{jl} d_{ac} - \delta_{ac} \delta_{ik} d_{lj} + \delta_{ac} \delta_{il} d_{kj} \\ & - \delta_{ac} \delta_{jl} d_{ki} + \delta_{ac} \delta_{jk} d_{li}. \end{aligned} \tag{32}$$

A.2 ($N + 1$)-electron case

A.2.1 p/p block. The zeroth-order part is given by

$$\langle \Phi^a | \hat{D} | \Phi^b \rangle = d_{ab}, \tag{33}$$

while for a valid HF reference there is again no first-order contribution. The second-order contribution from the single commutator involving $\hat{\sigma}_1$ is given by

$$\langle \Phi^a | [\hat{D}, \hat{\sigma}_1] | \Phi^b \rangle = -\sum_k \left(d_{ka} s_{kb} + d_{bk} s_{ka}^* \right). \tag{34}$$

The different contributions stemming from the double commutator involving $\hat{\sigma}_2$ are given by

$$\begin{aligned} \langle \Phi^a | [[\hat{D}, \hat{\sigma}_2], \hat{\sigma}_2] | \Phi^b \rangle = & -\frac{1}{4} \sum_{klcd} d_{cb} s_{klcd}^* s_{klad} \\ & -\frac{1}{4} \sum_{klcd} d_{ac} s_{klbd}^* s_{klcd} \\ & +\frac{1}{2} \sum_{klcd} d_{cd} s_{klcb}^* s_{klda} \\ & +\sum_{klmc} d_{lk} s_{kmcb}^* s_{lmca}. \end{aligned} \tag{35}$$

A.2.2 p/2p1h block. For the coupling block, the zeroth-order contribution is given by

$$\langle \Phi^a | \hat{D} | \Phi_j^{bc} \rangle = \delta_{ab} d_{jc} - \delta_{ac} d_{jb}, \tag{36}$$

while the first-order contributions are given by

$$\begin{aligned} \left\langle \Phi^a \middle| [\hat{D}, \hat{\sigma}_2] \middle| \Phi_j^{bc} \right\rangle = & \delta_{ab} \sum_{ld} d_{dl} s_{ljdc}^* \\ & - \delta_{ac} \sum_{ld} d_{jb} s_{ljdb}^* + \sum_l d_{al} s_{ljbc}^*. \end{aligned} \tag{37}$$

Again, the other coupling block is the Hermitian conjugate of this one.

A.2.3 2p1h/2p1h block. This block is again only needed in zeroth order, where the corresponding terms are given by

$$\begin{aligned} \left\langle \Phi_i^{ab} \middle| \hat{D} \middle| \Phi_j^{cd} \right\rangle = & \delta_{bd} \delta_{ij} d_{ac} - \delta_{bc} \delta_{ij} d_{ad} + \delta_{ac} \delta_{ij} d_{bd} \\ & - \delta_{ad} \delta_{ij} d_{bc} - \delta_{ac} \delta_{bd} d_{ji}. \end{aligned} \tag{38}$$

It should be noted that all these terms are in fact equivalent to the ones obtained in the intermediate state representation of a general one-particle operator within the perturbative algebraic-diagrammatic construction scheme.[42] This means, if the converged $\hat{\sigma}_1$ and $\hat{\sigma}_2$ cluster amplitudes are replaced by

Open Access Article. Published on 30 June 2025. Downloaded on 3/16/2026 4:00:36 PM.
This article is licensed under a Creative Commons Attribution 3.0 Unported Licence.

their second- and first-order analogues, $\hat{\sigma}_1^{(2)}$ and $\hat{\sigma}_2^{(1)}$, respectively, the resulting matrix elements are identical, analogous to the secular matrix $\overset{\approx}{\mathbf{M}}$ itself.[63,64]

Acknowledgements

M. H. acknowledges funding by the German Research Foundation (Deutsche Forschungsgemeinschaft, DFG) within the Walter Benjamin Program (grant no. 492735509). A. L. D. acknowledges funding by the German Research Foundation through grant no. 493826649.

Notes and references

1 J. C. Rienstra-Kiracofe, G. S. Tschumper, H. F. Schaefer, S. Nandi and G. B. Ellison, *Chem. Rev.*, 2002, **102**, 231–282.
2 A. Dreuw and L. S. Cederbaum, *Chem. Rev.*, 2002, **102**, 181–200.
3 J. Simons, *J. Phys. Chem. A*, 2008, **112**, 6401–6511.
4 B. Kippelen and J.-L. Brédas, *Energy Environ. Sci.*, 2009, **2**, 251–261.
5 J. L. Delgado, P.-A. Bouit, S. Filippone, M. Á. Herranz and N. Martín, *Chem. Commun.*, 2010, **46**, 4853–4865.
6 N. M. O'Boyle, C. M. Campbell and G. R. Hutchison, *J. Phys. Chem. C*, 2011, **115**, 16200–16210.
7 K. D. Jordan and P. D. Burrow, *Chem. Rev.*, 1987, **87**, 557–588.
8 J. Simons, *Annu. Rev. Phys. Chem.*, 2011, **62**, 107–128.
9 D. Davis, V. P. Vysotskiy, Y. Sajeev and L. S. Cederbaum, *Angew. Chem., Int. Ed.*, 2011, **50**, 4119–4122.
10 T. Sommerfeld, B. Bhattarai, V. P. Vysotskiy and L. S. Cederbaum, *J. Chem. Phys.*, 2010, **133**, 114301.
11 V. K. Voora and K. D. Jordan, *J. Phys. Chem. Lett.*, 2015, **6**, 3994–3997.
12 V. K. Voora, A. Kairalapova, T. Sommerfeld and K. D. Jordan, *J. Chem. Phys.*, 2017, **147**, 214114.
13 A. L. Fetter and J. D. Walecka, *Quantum Theory of Many-Particle Systems*, McGraw-Hill Book Company, New York, 1971.
14 L. S. Cederbaum and W. Domcke, *Adv. Chem. Phys.*, 1977, **36**, 205–344.
15 J. Simons, *Annu. Rev. Phys. Chem.*, 1977, **28**, 15–45.
16 J. Oddershede, *Adv. Quantum Chem.*, 1978, **11**, 275–352.
17 M. F. Herman, K. F. Freed and D. L. Yeager, *Adv. Chem. Phys.*, 1981, **48**, 1–69.
18 Y. Öhrn and G. Born, *Adv. Quantum Chem.*, 1981, **13**, 1–88.
19 W. von Niessen, J. Schirmer and L. S. Cederbaum, *Comput. Phys. Rep.*, 1984, **1**, 57–125.
20 L. S. Cederbaum, W. Domcke, J. Schirmer and W. von Niessen, *Adv. Chem. Phys.*, 1986, **65**, 115–159.
21 J. V. Ortiz, in *The Electron Propagator Picture of Molecular Electronic Structure*, ed. J. Leszczynski, World Scientific, Singapore, 1st edn, 1997, ch. 1, pp. 1–61.
22 D. Danovich, *Wiley Interdiscip. Rev.:Comput. Mol. Sci.*, 2011, **1**, 377–387.
23 H. H. Corzo and J. V. Ortiz, *Adv. Quantum Chem.*, 2017, **74**, 267–298.
24 J. Schirmer, *Many-Body Methods for Atoms, Molecules and Clusters*, Springer International Publishing, Heidelberg, 1st edn, 2018, vol. 94.
25 J. V. Ortiz, *Wiley Interdiscip. Rev.:Comput. Mol. Sci.*, 2013, **3**, 123–142.
26 E. Opoku, F. Pawłowski and J. V. Ortiz, *J. Phys. Chem. A*, 2024, **128**, 4730–4749.
27 J. Schirmer, L. S. Cederbaum and O. Walter, *Phys. Rev. A:At., Mol., Opt. Phys.*, 1983, **28**, 1237–1259.
28 G. Angonoa, O. Walter and J. Schirmer, *J. Chem. Phys.*, 1987, **87**, 6789–6801.
29 J. Schirmer and G. Angonoa, *J. Chem. Phys.*, 1989, **91**, 1754–1761.
30 L. S. Cederbaum, *J. Phys. B: At. Mol. Phys.*, 1975, **8**, 290–303.
31 V. G. Zakrzewski and J. V. Ortiz, *Int. J. Quantum Chem.*, 1995, **53**, 583–590.
32 J. V. Ortiz, *J. Chem. Phys.*, 1996, **104**, 7599–7605.
33 J. V. Ortiz, *J. Chem. Phys.*, 1998, **108**, 1008–1014.
34 J. Schirmer, A. B. Trofimov and G. Stelter, *J. Chem. Phys.*, 1998, **109**, 4734–4744.
35 A. B. Trofimov and J. Schirmer, *J. Chem. Phys.*, 2005, **123**, 144115.
36 J. Schirmer, *Phys. Rev. A:At., Mol., Opt. Phys.*, 1991, **43**, 4647–4659.
37 F. Mertins and J. Schirmer, *Phys. Rev. A:At., Mol., Opt. Phys.*, 1996, **53**, 2140–2152.
38 F. Mertins, J. Schirmer and A. Tarantelli, *Phys. Rev. A:At., Mol., Opt. Phys.*, 1996, **53**, 2153–2168.
39 D. Mukherjee and W. Kutzelnigg, Lecture Notes in Chemistry in *Many-Body Methods in Quantum Chemistry*, ed. U. Kaldor, Springer-Verlag, Heidelberg, 1989, vol. 52, pp. 257–274.
40 A. Y. Sokolov, *J. Chem. Phys.*, 2018, **149**, 204113.
41 S. Banerjee and A. Y. Sokolov, *J. Chem. Phys.*, 2019, **151**, 224112.
42 J. Schirmer and A. B. Trofimov, *J. Chem. Phys.*, 2004, **120**, 11449–11464.
43 A. L. Dempwolff, A. C. Paul, A. M. Belogolova, A. B. Trofimov and A. Dreuw, *J. Chem. Phys.*, 2020, **152**, 024113.
44 A. L. Dempwolff, A. C. Paul, A. M. Belogolova, A. B. Trofimov and A. Dreuw, *J. Chem. Phys.*, 2020, **152**, 024125.
45 A. L. Dempwolff, A. M. Belogolova, A. B. Trofimov and A. Dreuw, *J. Chem. Phys.*, 2021, **154**, 104117.
46 J. F. Stanton and R. J. Bartlett, *J. Chem. Phys.*, 1993, **98**, 7029–7039.
47 J. Schirmer and F. Mertins, *Int. J. Quantum Chem.*, 1996, **58**, 329–339.
48 A. I. Krylov, *Annu. Rev. Phys. Chem.*, 2008, **59**, 433–462.
49 I. Shavitt and R. J. Bartlett, *Many-Body Methods in Chemistry and Physics: MBPT and Coupled-Cluster Theory*, Cambridge University Press, Cambridge, 2009.
50 R. J. Bartlett, *Wiley Interdiscip. Rev.:Comput. Mol. Sci.*, 2012, **2**, 126–138.
51 J. Schirmer and F. Mertins, *Theor. Chem. Acc.*, 2010, **125**, 145–172.

 This journal is © the Owner Societies 2025

Open Access Article. Published on 30 June 2025. Downloaded on 3/16/2026 4:00:36 PM.
This article is licensed under a Creative Commons Attribution 3.0 Unported Licence.

52 T. D. Crawford and H. F. Schaefer III, *Rev. Comput. Chem.*, 2000, **14**, 33–136.
53 W. Kutzelnigg, *J. Chem. Phys.*, 1982, **77**, 3081–3097.
54 K. Tanaka and H. Terashima, *Chem. Phys. Lett.*, 1984, **106**, 558–562.
55 M. R. Hoffmann and J. Simons, *J. Chem. Phys.*, 1988, **88**, 993–1002.
56 M. D. Prasad, S. Pal and D. Mukherjee, *Phys. Rev. A:At., Mol., Opt. Phys.*, 1985, **31**, 1287–1298.
57 R. J. Bartlett, S. A. Kucharski and J. Noga, *Chem. Phys. Lett.*, 1989, **155**, 133–140.
58 R. J. Bartlett, S. A. Kucharski, J. Noga, J. D. Watts and G. W. Trucks, *Many-Body Methods in Quantum Chemistry*, Berlin, Heidelberg, 1989, pp. 125–149.
59 P. G. Szalay, M. Nooijen and R. J. Bartlett, *J. Chem. Phys.*, 1995, **103**, 281–298.
60 A. G. Taube and R. J. Bartlett, *Int. J. Quantum Chem.*, 2006, **106**, 3393–3401.
61 M. Hodecker, A. L. Dempwolff, J. Schirmer and A. Dreuw, *J. Chem. Phys.*, 2022, **156**, 074104.
62 G. Wälz, D. Kats, D. Usvyat, T. Korona and M. Schütz, *Phys. Rev. A:At., Mol., Opt. Phys.*, 2012, **86**, 052519.
63 J. Liu, A. Asthana, L. Cheng and D. Mukherjee, *J. Chem. Phys.*, 2018, **148**, 244110.
64 M. Hodecker, D. R. Rehn and A. Dreuw, *J. Chem. Phys.*, 2020, **152**, 094106.
65 M. Hodecker, S. M. Thielen, J. Liu, D. R. Rehn and A. Dreuw, *J. Chem. Theory Comput.*, 2020, **16**, 3654–3663.
66 M. Hodecker, A. L. Dempwolff, D. R. Rehn and A. Dreuw, *J. Chem. Phys.*, 2019, **150**, 174104.
67 M. Hodecker, D. R. Rehn, P. Norman and A. Dreuw, *J. Chem. Phys.*, 2019, **150**, 174105.
68 M. Hodecker and A. Dreuw, *J. Chem. Phys.*, 2020, **153**, 084112.
69 S. M. Thielen, M. Hodecker, J. Piazolo, D. R. Rehn and A. Dreuw, *J. Chem. Phys.*, 2021, **154**, 154108.
70 A. L. Dempwolff, M. Hodecker and A. Dreuw, *J. Chem. Phys.*, 2022, **156**, 054114.
71 M. Nooijen and R. J. Bartlett, *J. Chem. Phys.*, 1995, **102**, 3629–3647.
72 A. Szabo and N. S. Ostlund, *Modern Quantum Chemistry: Introduction to Advanced Electronic Structure Theory*, Dover, Mineola, New York, 1996.
73 E. Epifanovsky, A. T. B. Gilbert, X. Feng, J. Lee, Y. Mao, N. Mardirossian, P. Pokhilko, A. F. White, M. P. Coons, A. L. Dempwolff, Z. Gan, D. Hait, P. R. Horn, L. D. Jacobson, I. Kaliman, J. Kussmann, A. W. Lange, K. U. Lao, D. S. Levine, J. Liu, S. C. McKenzie, A. F. Morrison, K. D. Nanda, F. Plasser, D. R. Rehn, M. L. Vidal, Z.-Q. You, Y. Zhu, B. Alam, B. J. Albrecht, A. Aldossary, E. Alguire, J. H. Andersen, V. Athavale, D. Barton, K. Begam, A. Behn, N. Bellonzi, Y. A. Bernard, E. J. Berquist, H. G. A. Burton, A. Carreras, K. Carter-Fenk, R. Chakraborty, A. D. Chien, K. D. Closser, V. Cofer-Shabica, S. Dasgupta, M. de Wergifosse, J. Deng, M. Diedenhofen, H. Do, S. Ehlert, P.-T. Fang, S. Fatehi, Q. Feng, T. Friedhoff, J. Gayvert, Q. Ge, G. Gidofalvi, M. Goldey, J. Gomes, C. E. González-Espinoza, S. Gulania, A. O. Gunina, M. W. D. Hanson-Heine, P. H. P. Harbach, A. Hauser, M. F. Herbst, M. Hernández Vera, M. Hodecker, Z. C. Holden, S. Houck, X. Huang, K. Hui, B. C. Huynh, M. Ivanov, Á. Jász, H. Ji, H. Jiang, B. Kaduk, S. Kähler, K. Khistyaev, J. Kim, G. Kis, P. Klunzinger, Z. Koczor-Benda, J. H. Koh, D. Kosenkov, L. Koulias, T. Kowalczyk, C. M. Krauter, K. Kue, A. Kunitsa, T. Kuś, I. Ladjánszki, A. Landau, K. V. Lawler, D. Lefrancois, S. Lehtola, R. R. Li, Y.-P. Li, J. Liang, M. Liebenthal, H.-H. Lin, Y.-S. Lin, F. Liu, K.-Y. Liu, M. Loipersberger, A. Luenser, A. Manjanath, P. Manohar, E. Mansoor, S. F. Manzer, S.-P. Mao, A. V. Marenich, T. Markovich, S. Mason, S. A. Maurer, P. F. McLaughlin, M. F. S. J. Menger, J.-M. Mewes, S. Mewes, P. Morgante, J. W. Mullinax, K. J. Oosterbaan, G. Paran, A. C. Paul, S. K. Paul, F. Pavošević, Z. Pei, S. Prager, E. I. Proynov, Á. Rák, E. Ramos-Cordoba, B. Rana, A. E. Rask, A. Rettig, R. M. Richards, F. Rob, E. Rossomme, T. Scheele, M. Scheurer, M. Schneider, N. Sergueev, S. M. Sharada, W. Skomorowski, D. W. Small, C. J. Stein, Y.-C. Su, E. J. Sundstrom, Z. Tao, J. Thirman, G. J. Tornai, T. Tsuchimochi, N. M. Tubman, S. P. Veccham, O. Vydrov, J. Wenzel, J. Witte, A. Yamada, K. Yao, S. Yeganeh, S. R. Yost, A. Zech, I. Y. Zhang, X. Zhang, Y. Zhang, D. Zuev, A. Aspuru-Guzik, A. T. Bell, N. A. Besley, K. B. Bravaya, B. R. Brooks, D. Casanova, J.-D. Chai, S. Coriani, C. Cramer, G. Cserey, A. E. DePrince III, R. A. DiStasio Jr., A. Dreuw, B. D. Dunietz, T. R. Furlani, W. A. Goddard III, S. Hammes-Schiffer, T. Head-Gordon, W. J. Hehre, C.-P. Hsu, T.-C. Jagau, Y. Jung, A. Klamt, J. Kong, D. S. Lambrecht, W. Liang, N. J. Mayhall, C. W. McCurdy, J. B. Neaton, C. Ochsenfeld, J. A. Parkhill, R. Peverati, V. A. Rassolov, Y. Shao, L. V. Slipchenko, T. Stauch, R. P. Steele, J. E. Subotnik, A. J. W. Thom, A. Tkatchenko, D. G. Truhlar, T. Van Voorhis, T. A. Wesolowski, K. B. Whaley, H. L. Woodcock III, P. M. Zimmerman, S. Faraji, P. M. W. Gill, M. Head-Gordon, J. M. Herbert and A. I. Krylov, *J. Chem. Phys.*, 2021, **155**, 084801.
74 M. Wormit, D. R. Rehn, P. H. P. Harbach, J. Wenzel, C. M. Krauter, E. Epifanovsky and A. Dreuw, *Mol. Phys.*, 2014, **112**, 774–784.
75 E. Epifanovsky, M. Wormit, T. Kuś, A. Landau, D. Zuev, K. Khistyaev, P. Manohar, I. Kaliman, A. Dreuw and A. I. Krylov, *J. Comput. Chem.*, 2013, **34**, 2293–2309.
76 T. L. Stahl and A. Y. Sokolov, *J. Chem. Phys.*, 2024, **160**, 204104.
77 T. L. Stahl, S. Banerjee and A. Y. Sokolov, *J. Chem. Phys.*, 2022, **157**, 044106.